Available online at www.sciencedirect.com

ScienceDirect

Advances in Space Research 66 (2020) 2402–2415

ADVANCES IN SPACE RESEARCH (a COSPAR publication)

www.elsevier.com/locate/asr

Bio-inspired guidance method for a soft landing on a Near-Earth Asteroid

R. Valenzuela Najera, L. Everett, A.G. Ortega, A. Choudhuri, A. Flores-Abad *

Mechanical Engineering Department, The University of Texas at El Paso, El Paso, TX 79968, USA
Center for Space Exploration and Technology Research, The University of Texas at El Paso, El Paso, TX 79968, USA

Received 12 March 2020; received in revised form 16 July 2020; accepted 31 July 2020
Available online 13 August 2020

Abstract

Achieving a soft landing over the surface of small celestial bodies is an essential maneuver in space to advance the status of space exploration, sample collecting and in-situ resource utilization, among other on-orbit tasks. Landing on these bodies is challenging due to the reduced-gravity and airless environment. The correct planning of execution of the trajectory to land on the surface of the body is of cumbersome importance to prevent the vehicle from bouncing up and eventually reach escape velocity. In this paper, a bio-inspired trajectory planning method to land on the surface of a Near-Earth Asteroid (NEA) with zero relative velocity is proposed. The method is based on Tau theory, which has been demonstrated to explain the way that humans and some other animals' approach to different target spots to perform tasks such as perching, landing, and grasping. We have selected the NEA Apophis asteroid as our case study due to its accessibility, and small rotational velocity and orbit condition code. Two landing scenarios are studied; one considers the case where the satellite is hovering at a low altitude; the other corresponds to a landing maneuver right after a deorbiting or breaking phase, which may cause residual initial velocity in the vehicle prior to the landing maneuver. Once the descending trajectory is obtained, a closed-loop controller is in charge of achieving trajectory tracking and calculating the continuous and on/off thrust control signals. The simulation results show that the introduced approach can achieve zero final relative velocity in both cases for different initial condition, which is a requirement for a soft landing. Besides, different kinematic behaviors can be obtained by modifying the single variable named the Tau constant. The particular advantages of the method with respect to a commonly used approach are devised and analyzed as well.
Published by Elsevier Ltd on behalf of COSPAR.

Keywords: Guidance; Asteroid Landing; Bio-inspired

1. Introduction

Small celestial bodies such as asteroids and comets are of growing attention because they can provide insights of the formation and evolution of the solar system. From the numerous small bodies in outer space, Near-Earth Asteroids (NEA) are of interest due to their accessibility and Earth collision threat. Besides, NEA might pose material resources that can help to maintain space exploration sustainable. Landing on NEA to further obtain a sample is a challenging task mainly because of the airless and reduced-gravity environment, which may cause uncontrolled bounce if the trajectory is not properly planned. Many missions from the different space agencies have been launched to land in asteroids and comets. For example, NASA's Shoemaker (Veverka et al. 2001), JAXA's Hayabusa (Yoshimitsu et al., 2006; Yano et al., 2006) and Hayabusa2 (Tsuda et al., 2019), ESA's Rosetta (Accomazzo et al., 2017) and OSIRIS-Rex (Lauretta et al., 2015). However, despite of the fact that Minerva and Philae (Biele et al., 2015), the corresponding lander modules of

* Corresponding author.
E-mail address: afloresabad@utep.edu (A. Flores-Abad).

https://doi.org/10.1016/j.asr.2020.07.048
0273-1177/Published by Elsevier Ltd on behalf of COSPAR.

the missions, touched the surface of the celestial bodies, a firm and stable landing was not achieved due to different factors. More recently, the Hayabusa2 spacecraft has been sent to its journey to Asteroid Ryugu. Hayabusa2 also features a lander package termed MASCOT. With the objective of successfully landing on a small celestial body, the trajectory to follow must be planned properly (Huang et al., 2004). To advance towards the correct development of this challenging tasks, the community has introduced different methods to guide a spacecraft to achieve a soft landing. In Huang et al. (2004), Li et al. (2006), Lan et al. (2014), the authors proposed autonomous guidance methods where the landing process was transformed into the trajectory tracking of a curve given by a cubic polynomial. Some optimal trajectories have also been proposed to reduce fuel (Lantoine and Braun, 2006; Yang and Baoyin, 2015; Yang et al., 2019; Cheng et al., 2019, Yang and Li, 2020), for example advanced closed-loop techniques such as sliding modes (Zezu et al., 2012; Yang et al., 2017a, 2017b), fuzzy logic (Li et al., 2015) and predictive control (AlandiHallaj and Assadian, 2017), among others. Ballistic trajectories have also been proposed to land on asteroids, for example (Tardivel and Scheeres, 2013) employed an adaptable, and robust method for ballistic landings on the surface of a binary asteroid to deploy a lander from a mother spacecraft using a passive trajectory; (Ferrari and Lavagna,2018) designed a ballistic landing trajectory, where manifold dynamics are exploited to find low-energy trajectories; while (Tardivel et al., 2013) proposed a ballistic trajectory to deploy a light lander on asteroid (175706) 1996 FG. (Ferrari et al., 2016) used a patched three-body strategy to model the dynamics around the binary couple, using different three-body problems.

The guidance phase in most of the previous works is based on a spline defined by cubic polynomials. However, this technique have some drawbacks that may cause landing problems when used to guide of spacecraft for landing purposes. For example, a small deviation and/or uncertainty on the initial conditions of the maneuver will result in an erroneous calculation of the polynomial parameters and as a result the landing position may not be exactly reached, or the desired final velocity can be also deviated.

Convex optimization involves minimizing a convex objective function and include the subclasses of linear programing, second-order cone program (SOCP), quadratic program, and least squares. Recent publications show that convex optimization techniques have been used to generate a landing trajectory on an asteroid minimizing fuel consumption and descent flight time (Pinson and Lu, 2015; Yang et al., 2017a, 2017b; Pinson and Lu, 2018). In this regard, a convex function is defined to connect two points by posing the optimization problem in a second-order cone function where inequality constraint would require all the values to lie inside or on the cone to solve the problem.

In this work, we analyze the use of a bio-inspired method based on Tau-theory (Lee, 2009), which explains the way that humans and some animals guide their extremities to reach a specific spot. Because humans and animals have improved their capabilities through the natural selection process, this approach is worthy of being studied to devise its applicability in the trajectory planning of a spacecraft landing on an asteroid. In Tau theory, it is explained that an animal or human naturally approach an object by closing gaps, these can be for example distance and orientation gaps. Since the gaps can all be close at the same time, the terminal conditions of the trajectory can be achieved, including zero or small relative velocity, if desired. To validate the approach; a simulation in 3D space is created to recreate a landing trajectory on the Apophis asteroid, which was selected due to its accessibility, diameter, large rotational period and small orbit condition code (NASA Jet Propulsion Laboratory, 2005). As general advantages of the method, it is identified that the tau-theory inspired approach is able to cope with desired and undesired changes in the boundary conditions and modifications in the kinematic (position, velocity and acceleration) behavior of the landing trajectory by simply modifying a single constant value, termed tau constant or tau-coupling constant, depending on the landing scenario. Consequently, the method has the potential to reduce the complexity in the design and implementation of the guidance law.

2. Problem statement

The paper addresses the orbital scenario where a lander spacecraft is orbiting or hovering above a small celestial body such as an asteroid. Then, at a given initial moment, t_0, a descent maneuver is commanded with the objective of achieving a soft landing so that the spacecraft does not escape the asteroid's gravitational field. To describe the kinematics and dynamics of the space vehicle, the reference

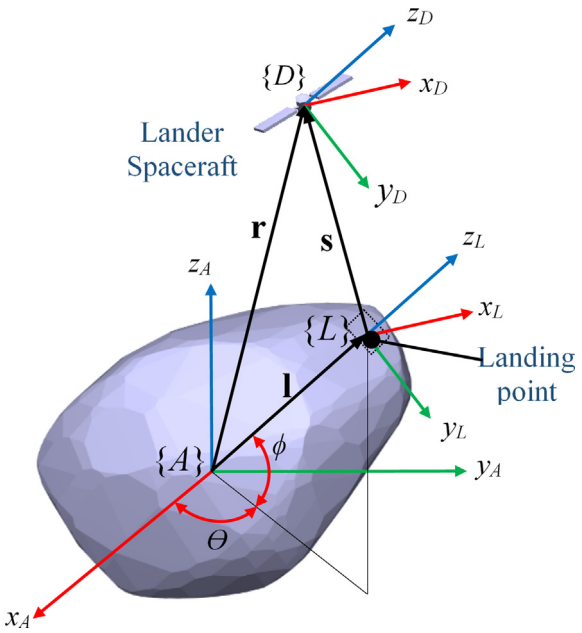

Fig. 1. Coordinate system definition in a reference frame.

frames depicted in Fig. 1 are defined. Consider that the origin of the coordinate system $\{L\}$ is at the selected landing site and that the z_L – axis matches the direction of vector $\mathbf{l}$, which has its origin at the asteroid's center of mass and goes to the landing point. Furthermore, let $\{A\}$ be the coordinate system with its origin fixed with the asteroid's center of mass. Besides, $\{D\}$ is located at the center of mass of the spacecraft.

2.1. Assumptions

To focus the work in the bio-inspired guidance approach, the introduced approach considers the following assumptions:

(a) Close-range rendezvous has been performed.
(b) The full state of the spacecraft is known, i.e., there exists a vision-based sensory system that mimics that of the living beings, which provides the position and velocity of the spacecraft relative to the asteroid.
(c) The trajectory tracking uses an active closed-loop autonomous controller.
(d) The mass parameters of the systems are also known and remain constant during the whole maneuver.
(e) Only the gravitational attraction of the second body is considered as the third and superiors provide a small contribution in comparison with the control forces exerted by the actuators.
(f) The asteroid is considered to have an ellipsoid shape with axes dimensions in accordance with the reported size of asteroid 99942 Apophis.

2.2. Dynamic modeling

The dynamic model for the spacecraft moving in the vicinity of rotating asteroid and under the influence of control accelerations and solar radiation disturbances can be expressed in the asteroid-centric Cartesian reference frame by (Li et al., 2006):

$$\ddot{\mathbf{r}} = \boldsymbol{a}_T + \nabla u + \boldsymbol{a}_{SRP} - 2\boldsymbol{\omega} \times \dot{\boldsymbol{r}} - \dot{\boldsymbol{\omega}} \times \boldsymbol{r} - \boldsymbol{\omega} \times (\boldsymbol{\omega} \times \boldsymbol{r}) \quad (1)$$

In the previous equation, $\boldsymbol{r} \in \mathbb{R}^{3\times1}$ represents position vector from mass center of the target asteroid to the spacecraft $\boldsymbol{a}_T \in \mathbb{R}^{3\times1}$ is the control acceleration vector provided by the thrusters, $\nabla u \in \mathbb{R}^{3\times1}$ the gradient of the gravitational potential function u, $\boldsymbol{a}_{SRP} \in {}^{3\times1}$ are disturbance vector caused by solar radiation pressure and $\boldsymbol{\omega} \in \mathbb{R}^{3\times1}$ the angular velocity vector of the asteroid. Considering the case where the asteroid is rotating about its maximum moment of inertia with the constant rate ω_a, the angular velocity vector is constant and $\dot{\omega}_a = 0$, then, we can simplify (1) to:

$$\ddot{\mathbf{r}} = \boldsymbol{a}_T + \nabla u + \boldsymbol{a}_{SRP} - 2\boldsymbol{\omega} \times \dot{\boldsymbol{r}} - \boldsymbol{\omega} \times (\boldsymbol{\omega} \times \boldsymbol{r}) \quad (2)$$

the z-axis is aligned with the maximum moment of inertia, the body-fixed reference frame motion equations can be written in its scalar components form as:

$$\begin{bmatrix} \ddot{x} \\ \ddot{y} \\ \ddot{z} \end{bmatrix} = \begin{bmatrix} 2\omega_a\dot{y} + \omega_a^2 x + ux + a_{Tx} + aSRPx \\ -2\omega_a\dot{x} + \omega_a^2 y + uy + a_{Ty} + aSRPy \\ uz + a_{Tz} + aSRPz \end{bmatrix} \quad (3)$$

2.3. Asteroid Model.

Among small celestial bodies, NEA's are of interest due to its accessibility and risk of colliding with the Earth. One of the asteroids that has attracted more interest in this regard is the asteroid 99942 Apophis (Ivashkin and Stikhno, 2009), which estimated geometry is shown in Fig. 2 (Frieger, 2013). Late studies show that there is low chance that Apophis collides with the Earth. However, it will still pass close to the Earth and as a such its accessibility is increased and different missions to flyby, rendezvous or landing are suitable to propose, which will help to gain a better understanding of the NEA. Some of the Apophis parameters provided by Pravec et al. (2014), Ivashkin and Lang (2017), TheSkyLive (2020) are shown in Table 1.

2.4. Gravity field

In this work, the attraction force exerted by the asteroid on the spacecraft in the landing maneuver is considered by using the general form for the spherical harmonic potential, the gravity field is given as (Balmino, 1994; Scheeres, 2012; Zhenjiang et al., 2012; Liu et al. 2014):

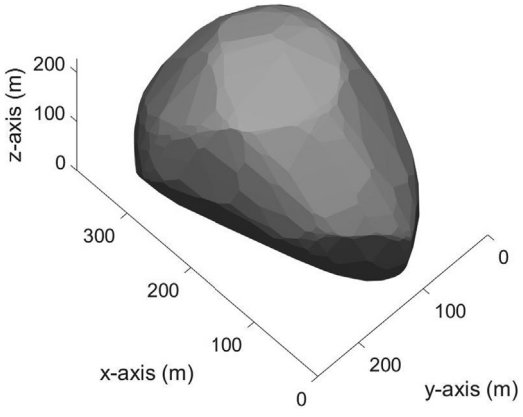

Fig. 2. Apophis asteroid model.

Table 1
Apophis properties.

Property	Value
Mean diameter	$d = 0.320$ km
Mass	$m_a = 4.3 \times 10^{10}$ kg
Ellipsoid semi-major axis	$\alpha = 0.370$ km
Ellipsoid semi-axis medium	$\beta = 1.06\ \Upsilon$
Ellipsoid semi-axis minor	$\Upsilon = \alpha/1.5$

$$u(r,\phi,\theta)=\frac{\mu}{r}\sum_{l=0}^{\infty}\sum_{m=0}^{l}\left(\frac{r_o}{r}\right)^{l}P_{lm}(\sin\phi)[C_{lm}\cos m\theta+S_{lm}\sin m\theta] \tag{4}$$

where

r,ϕ,θ : radius vector, latitude and longitude, respectively.
$\mu=GM$: gravitational parameter, where G is the gravitational constant and M the mass of the body.
r : distance from the mass center of small body to the spacecraft,
r_o : normalizing radius (often chosen as either the maximum radius or mean radius of the body),
P_{lm} : associated Legendre Functions,
C_{lm} and S_{lm} : gravity field harmonic coefficients.

Considering the asteroid is a constant density ellipsoid with semi-major axes $\gamma \leqslant \beta \leqslant \alpha$ (see Table 1), the simplified form of the gravity potential leads to (Scheeres, 2012):

$$u=\frac{\mu}{r}\left[1+\left(\frac{r_0}{r}\right)^{2}\left\{C_{20}(1-\frac{3}{2}\cos^2\phi)+3C_{22}\cos^2\phi\cos(2\theta)\right\}\right] \tag{5}$$

for which, the second order harmonic coefficients are:

$$\begin{aligned} C20&=\tfrac{1}{5\alpha^2}\left(\gamma-\tfrac{\alpha^2-\beta^2}{2}\right)\\ C22&=\tfrac{1}{20\alpha^2}\left(\alpha^2-\beta^2\right)\end{aligned} \tag{6}$$

and the partial derivatives of the potential are expressed as

$$\begin{aligned} \tfrac{\partial u}{\partial x}&=ux=-\tfrac{3\mu x}{2}\int_{\lambda(r)}^{\infty}\tfrac{du}{(\alpha^2+u)\Delta(u)}\\ \tfrac{\partial u}{\partial y}&=uy=-\tfrac{3\mu y}{2}\int_{\lambda(r)}^{\infty}\tfrac{du}{(\beta^2+u)\Delta(u)}\\ \tfrac{\partial u}{\partial z}&=uz=-\tfrac{3\mu z}{2}\int_{\lambda(r)}^{\infty}\tfrac{du}{(\gamma^2+u)\Delta(u)}\end{aligned} \tag{7}$$

with x, y, z being Cartesians coordinates, the parameter $\lambda(r)=0$ on the lower limit of the integration symbol, and the symbol ∞ on the upper limit means that gravitational field can extend over the entire small body surface.

2.5. Solar radiation pressure

The solar radiation pressure is another important orbital disturbance for missions to small bodies. This work considers a simple model to calculate the acceleration due to solar radiation where the spacecraft is supposed to have a constant area perpendicular to the solar line and the incident radiation is reflected. Since the spacecraft is very close to the target asteroid the magnitude of the solar radiation pressure acceleration can be expressed as (Scheeres, 2012):

$$\boldsymbol{a}_{SRP}=-\frac{(1+\rho)Po}{B_{sc}\boldsymbol{d}^2} \tag{8}$$

ρ: Total reflection of the spacecraft,
P_0: Solar constant approximately equal to $1\text{x}10^8$ kg km^3/s^{2}m^2
A_{sc}: The reflection area of the spacecraft
M_{sc}: The mass of the spacecraft
$B_{sc}=M_{sc}/A_{\text{sc}}$
$\boldsymbol{d}$: Distance vector from the asteroid to the sun

3. The bio-inspired trajectory planning method

Landing on a small celestial body is still very challenging and requires adequate guidance and control strategies to properly design the trajectory and track it during the maneuver to achieve a zero or small relative velocity between the spacecraft and the asteroid landing point. The objective of this section is to develop a trajectory generation method based on the time-to-contact principle of the General Tau theory, which is a theory that explain the guidance of bodily movements of humans and some animals.

3.1. Tau theory-based guidance

Tau theory generalized by Lee was developed from the work on J.J. Gibson (Lee, 2009) and explains how animals control their motion using visual feedback for different tasks including landing and perching. Tau theory is based on a concept called time-to-contact (Lee, 1976), which is the required time to reach an object if the current velocity is maintained. In 1998 Tau theory was extended by Lee introducing Tau-coupling which explain the movement synchronization closing gaps by means of the function tau $\tau(t)$ (Lee,1998). Some applications of the tau theory in motion control have been developed to control robots' motion (Zhang et al., 2017) and for similar tasks such as perching, docking, braking, or landing in unmanned aircraft systems (Kendoul and Ahmed, 2010; Kendoul, 2013; Zhang et al., 2014). This work proposes the use of extended Tau theory to generate a trajectory for soft landing on an asteroid.

The general theory encompasses perception and movement and is based on some fundamental principles (Lee, 1998):

1. The main task in guiding intentional motion is to control the closure of spatial and/or force action gaps (or simply gaps) $\chi(t)$ between end-effectors, or sensory organs, and their goals.
2. This requires sensing the closures of gaps in sensory inputs arrays, for example optical (vision), acoustic (echolocating bats), force (haptics), electrical (electrolocation fish), and electromagnetic (infrared detection by snakes)
3. The tau $\tau(t)$ of each spatial and/or force gap be expressed as the first-order time-to-closure of the action-gap at the current rate of closure, i.e.

$$\tau(t) = \frac{\chi(t)}{\dot{\chi}(t)} \tag{9}$$

4. A principal method of movement guidance is by coupling the taus of different action-gaps, that is keeping the taus in constant ratio during a movement.

The overall objective of the landing maneuver is to reach the target point with zero velocity and zero acceleration at the contact moment. In the particular case of the landing maneuver, the main purpose would be to close the motion gap described by the position vector $\boldsymbol{s}(t)$, for that, we will denote τ_x, τ_y and τ_z the corresponding taus to the gaps s_x, s_y and s_z, respectively. Therefore, in this scenario, we must close three position gaps defined by

$$\tau_x(t) = \frac{s_x(t)}{\dot{s}_x(t)}, \quad \tau_x(t) = \frac{s_y(t)}{\dot{s}_y(t)} \quad \text{and} \quad \tau_z(t) = \frac{s_z(t)}{\dot{s}_z(t)} \tag{10}$$

where $s_x(t)$, $s_y(t)$, and $s_z(t)$ are the components of the position vector $\mathbf{s}(t)$. Note that the proposed landing trajectory could be generated considering two scenarios; one is the case of landing after an stable orbit-attitude hovering, where both the position and attitude of the spacecraft are kept to be stationary in the asteroid body-fixed frame, as a such we can consider that this is a zero-initial velocity scenario; the other case corresponds to that of an spacecraft orbiting and/or rotating with the asteroid in the inertial space, in this setting, the spacecraft may have a residual non-zero initial velocity (Wang and Xu, 2015; Santos et al., 2018) at the moment of performing the landing motion.

3.1.1. Case 1. After deorbiting – non-zero residual initial velocity

Assume that the spacecraft has reached a descent position after orbiting the asteroid and it is ready to land. In this case, it is possible to generate a descending trajectory with a small residual velocity, not necessary zero, that is to say $\dot{\boldsymbol{s}}(0) \neq 0$. Here, we can use Tau theory to control the closure of action gaps. Lee explains that the theory applies to approach along any dimension and that the only information necessary for an object to control a descent action is the tau time rate (Lee, 2009), which is given by the constant tau-dot:

$$\dot{\tau}_i(t) = k_i \tag{11}$$

where $i = x, y, z$ and k_i is a constant used in Tau theory to ensure the closing of gaps and reach the final target smoothly with zero relative velocity. The k values should remain within the range of $0 < k < 0.5$ to converge to a finite landing point with a small relative velocity (Lee et al., 1993). In the strategy of closing action gaps, any other value outside this range causes that the landing point is not reached or that it reaches the objective point at an uncontrolled speed generating a collision on the target (see Table 2).

Another important tau-guidance law to consider is given by:

$$\tau_i(t) = k_i t + \tau_{i_0} \tag{12}$$

where τ_{i_0}corresponds to tau when $t = 0$ at the moment when tau-action is initiated, which in turn is defined by:

$$\tau_{i_0} = \frac{s_{i_0}}{\dot{s}_{i_0}} \tag{13}$$

where $s_{i_0}$and $\dot{s}_{i_0}$ are the initial position and velocity of the spacecraft in the corresponding i direction. Combining Eqs. (9), (11) and (12), we can solve for $s_z(t)$, $\dot{s}_z(t)$, and $\ddot{s}_z(t)$ to obtain the close-of-the-action-gap motion equations in the altitude direction.

$$s_z(t) = s_{z_0}\left(1 + k_z t \frac{\dot{s}_{z_0}}{s_{z_0}}\right)^{\frac{1}{k_z}} \tag{14}$$

$$\dot{s}_z(t) = \dot{s}_{z_0}\left(1 + k_z t \frac{\dot{s}_{z_0}}{s_{z_0}}\right)^{\frac{1-k_z}{k_z}} \tag{15}$$

$$\ddot{s}_z(t) = \frac{\dot{s}_{z_0}^2}{s_{z_0}}(1 - k_z)\left(1 + k_z t \frac{\dot{s}_{z_0}}{s_{z_0}}\right)^{\frac{1-2k_z}{k_z}} \tag{16}$$

From the above equations, *"Tau Action Gap"*, which describe the movement of a biological entity moving with a given initial velocity until reaching a target smoothly with zero relative velocity, $\dot{z}(t), and\ \ddot{z}(t)$ will become zero at the same finite time t. Considering, $s_{z_0} = 1450$ m, $s_{z_0} = -3.3$ m/s and $0 \leqslant t \leqslant 1200$ s, the position and velocity of an action gap were calculated at different values of k_z and are shown in Fig. 3, where we can see the behavior of the a) altitude, and b) velocity. One can observe that the movement converges to the target point smoothly and with zero final velocity only for some value in $0 < k_z < 0.5$.

Since our trajectory design needs to be performed considering a 3D (3-dimensional) environment, it is necessary to expand the closing of action gaps in the three coordinate axes x, y and z. To achieve such a trajectory, it is impera-

Table 2
Tau strategy motion: k-values-final status.

Tau Action-Gap	Tau-coupling	Intrinsic-Tau
$k_i < 0$.....Gap not close	$k_{iz} < 0$.....Gap x not close	$k_{ig} < 0$.....Gap not close
$k_i = 0$.....Gap not close	$k_{iz} = 0$.....Nonsense	$k_{ig} = 0$.....Nonsense
$0 < k_i < 0.5$.....Achieve goal	$0 < k_{iz} \leqslant 0.5$.....Achieve goal	$0 < k_{ig} < 0.5$.....Achieve goal
$k_i = 0.5$.....Slight collision	$0.5 < k_{iz} < 1$.....Slight collision	$0.5 < k_{ig} < 1$.....Slight collision
$0.5 < k_i < 1$.....Slight collision	$k_{iz} = 1$.....Achieve goal	$k_{ig} = 1$.....Achieve goal
$k_i = 1$.....Strong collision	$k_{iz} > 1$.....Strong collision	$k_{ig} > 1$.....Strong collision
$k_i > 1$.....Strong collision		

tive to use the *tau-coupling* strategy, which establishes that multiple gaps – such as controlling the direction and speed of approach – need to be closed simultaneously to synchronize the maneuver. One option to guide the movements and the closing of gaps is by using tau-coupling of τ_x, τ_y and τ_z during the movement expressed by:

$$\tau_x = k_{xz}\tau_z \tag{17}$$

$$\tau_y = k_{yz}\tau_z \tag{18}$$

where k_{xz} and k_{yz} are constants that governs the kinematics of closure of gap x and $y$respectively. It can be shown that if their values are selected correctly, the variables $(x,\dot{x},\ddot{x})$, $(y,\dot{y},\ddot{y})$ and $(z,\dot{z},\ddot{z})$ become zero at the same time. This condition was presented by Lee (1998), where mathematically he demonstrates the synchronization of the guided movements as:

$$s_x = A s_z^{\frac{1}{k_{xz}}} \tag{19}$$

$$\dot{s}_x = \frac{A}{k_{xz}} s_z^{\frac{1}{k_{xz}}-1}\dot{s}_z \tag{20}$$

$$\ddot{s}_x = \frac{A}{k_{xz}} s_z^{\frac{1}{k_{xz}}-2}\left(\frac{1-k_{xz}}{k_{xz}}\dot{s}_z^2 + s_z\ddot{s}_z\right) \tag{21}$$

$$A = \frac{s_{x_0}}{s_{z_0}^{1/k_{xz}}} \tag{22}$$

The same operation to determine the position, velocity, and acceleration on the $y-$axis.

$$s_y = B s_z^{\frac{1}{k_{yz}}} \tag{23}$$

$$\dot{s}_y = \frac{B}{k_{yz}} s_z^{\frac{1}{k_{yz}}-1}\dot{s}_z \tag{24}$$

$$\ddot{s}_y = \frac{B}{k_{yz}} s_z^{\frac{1}{k_{yz}}-2}\left(\frac{1-k_{yz}}{k_{yz}}\dot{s}_z^2 + s_z\ddot{s}_z\right) \tag{25}$$

$$B = \frac{s_{y_0}}{s_{z_0}^{1/k_{yz}}} \tag{26}$$

3.1.2. Case 2. Hovering – zero initial velocity

When the objective of the movement is to close multiple gaps at a given time of arrival t_g from a static initial state (Lee, 1998), such as the case of landing from near-inertial hovering position. In this scenario, the movement starts at rest, accelerates and then slows down until the end of the movement reaching the position again at zero-speed and zero-acceleration. The movements are intrinsically guided by Tau coupling the gap $s_i(t)$ and the intrinsically guiding gaps are represented by:

$$\tau_i(t) = k_{ig}\tau_{ig}(t) \tag{27}$$

where k_{ig} is a positive constant value that determines the kinematics of the movement for $i = x,y,z$, and $\tau_{ig}(t)$ is a function of time that specifies the time of the gap to be closed as (Lee, 1998):

$$\tau_{ig}(t) = \frac{s_{i_g}(t)}{\dot{s}_{i_g}(t)} = \frac{1}{2}\left(t - \frac{t_g^2}{t}\right) \tag{28}$$

where t_g is the total duration time of the maneuver and t runs from 0 to t_g. By using Eq. (28) and substituting in Eqs. (11) and (12) we obtain the first order differential equation:

$$\dot{s}_i(t) + \frac{-1}{k_{ig}\frac{1}{2}\left(t - \frac{t_g^2}{t}\right)} s_i(t) = 0 \tag{29}$$

for which the solution for $s_z(t)$ is:

$$s_z(t) = \frac{s_{z_0}}{t_g^{2/k_{zg}}}\left(t_g^2 - t^2\right)^{\frac{1}{k_{zg}}} \tag{30}$$

$$\dot{s}_z(t) = \frac{-2s_{z_0}t}{k_{zg}t_g^{2/k_{zg}}}\left(t_g^2 - t^2\right)^{\frac{1}{k_{zg}}-1} \tag{31}$$

$$\ddot{s}_z(t) = \frac{2s_{z_0}}{k_{zg}t_g^{2/k_{zg}}}\left(\frac{2t^2}{k_{zg}} - t^2 - t_g^2\right)\left(t_g^2 - t^2\right)^{\frac{1}{k_{zg}}-2} \tag{32}$$

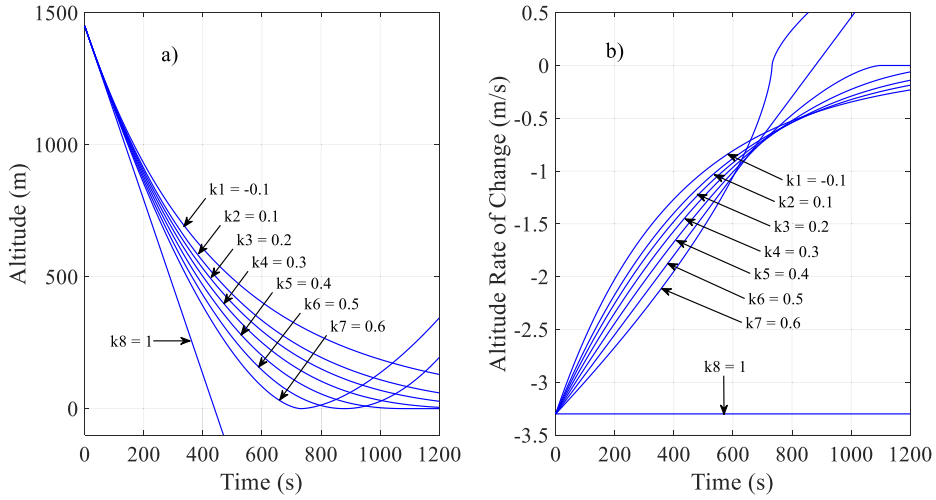

Fig. 3. Tau action-gap, (a) position, (b) velocity, at different k-values.

Eqs. (30)–(32) represent the position, velocity and acceleration respectively for the guided motion closing the intrinsic gap. Fig. 4 shows altitude and velocity time history for different k-values.

3.1.3. Optimal tau-constant k values

The numerical values of the constant k can also be extracted from Table 2, which shows a list of data obtained from the analysis of the consequences of the movement at different values of k for each of the tau theory strategies (Zhang et al., 2014).

From Table 2, we observe that there are different options to choose for the value of k. In order to have a good performance of the maneuver, we can find an optimal value for k that allows using the less amount of energy or minimizing the time to landing, or any other objective function. Here, we propose to find the k value that achieves the minimum travel distance. Thus, the optimal value of the constant k can be calculated by solving a nonlinear constrained optimization problem. Therefore, we define the trajectory vector function $\boldsymbol{s}(t,k)$ that connects $\{D\}$ with $\{L\}$ (see Fig. 1) as (Dawkins, 2003):

$$\boldsymbol{s}(t,k) = \langle s_x(t,k),\ s_y(t,k),\ s_z(t,k)\rangle \tag{33}$$

on the interval $t_0 \leqslant t \leqslant t_g$ has an arc length in 3D

$$\| \boldsymbol{s}(t,k) \| = \int_{t_0}^{t_g} \sqrt{\left[s_x'(t,k)\right]^2 + \left[s_y'(t,k)\right]^2 + \left[s_z'(t,k)\right]^2}\,dt \tag{34}$$

Here, we are particularly interested in the altitude (about the z-axis), in this case, we can determine the optimal value of k by defining the following optimization problem.

minimize:

$$\| \boldsymbol{s}_z(t,k) \| = \int_{t_0}^{t_g} \sqrt{1 + \left[s_z'(t,k_z)\right]^2}\,dt \tag{35}$$

subject to:

$$s_{z_0} = 1450 \text{ m}$$
$$\dot{s}_{z_0} = 3.3 \text{ m/s}$$
$$t_g = 1200 \text{ s}$$
$$0 < k_z < 0.5$$

The values for the constants k_x and k_y can be determined in the same way or selected from Table 2.

4. Trajectory tracking: coupled PD-PWPF controller

Once the desired trajectory has been defined, the design of a control algorithm able to track it is needed. Besides, the spacecraft engines requires an on-off discrete signal. For this purpose, since our objective is not to propose a control method, we employ a common PD controller to calculate the continuous control signal, which is further complemented with pulse width pulse frequency (PWPF) scheme to provide the required switching control signal to the thrusters. A block diagram of these coupled controllers is shown in Fig. 5.

The control law equation for the proportional control plus velocity feedback is given by:

$$\boldsymbol{s}_c(t) = \boldsymbol{K}_p\,\tilde{\boldsymbol{s}}\,(t) + \boldsymbol{K}_v\dot{\tilde{\boldsymbol{s}}}(t) \tag{36}$$

where $\boldsymbol{K}_p, \boldsymbol{K}_v \in \mathbb{R}^{3\times3}$ are the position and velocity (derivative) gain matrices (Kelly et al., 2005), the vector $\boldsymbol{s}_\tau \in \mathbb{R}^{3\times1}$ represents the spacecraft desired bioinspired trajectory, $\dot{\boldsymbol{s}}_\tau \in \mathbb{R}^{3\times1}$ is the velocity of the desired trajectory, the vector $\tilde{\boldsymbol{s}} = \boldsymbol{s}_\tau - \boldsymbol{s} \in \mathbb{R}^{3\times1}$ is the position error, and the vector $\dot{\tilde{\boldsymbol{s}}} = \dot{\boldsymbol{s}}_\tau - \dot{\boldsymbol{s}} \in \mathbb{R}^{3\times1}$ is the velocity error. The selected values for the gains $\boldsymbol{K}_p, \boldsymbol{K}_v$ are shown in Table 4. The magnitude of the force necessary for the spacecraft propulsion is represented in the controller by the control block PWPF commonly used by the thrusters for attitude control, it is shown in Fig. 6.

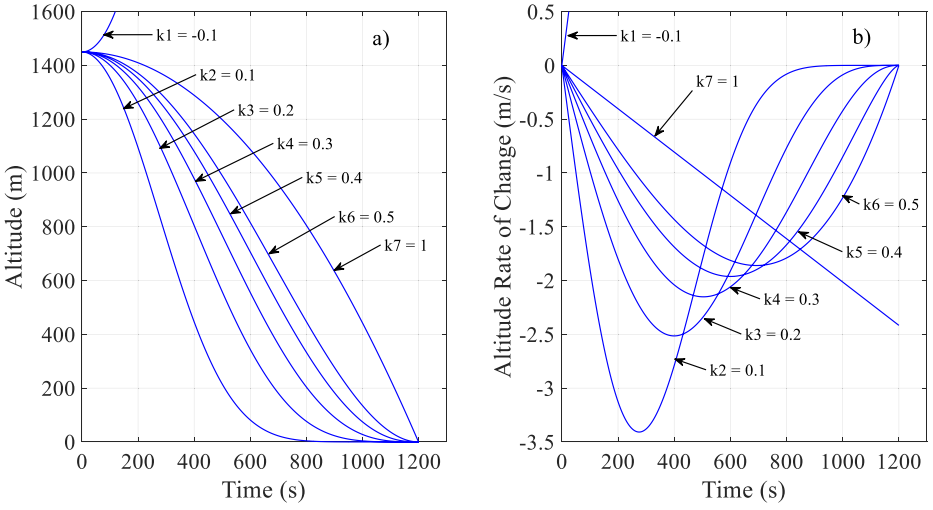

Fig. 4. Intrinsic -Tau guidance, (a) position, (b) velocity, at different k-values.

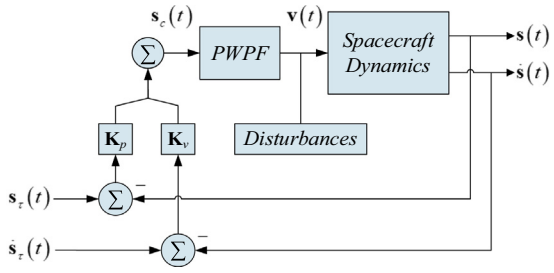

Fig. 5. PD-PWPF trajectory tracking control.

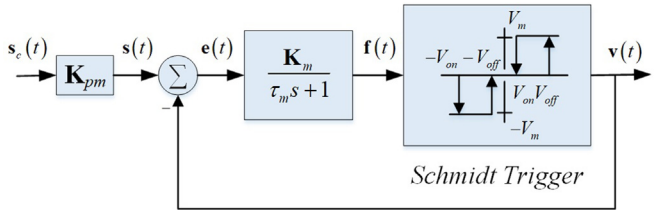

Fig. 6. Pulse-width pulse-frequency modulated system.

$\boldsymbol{K}_{pm} \in \mathbb{R}^{3\times3}$ is a constant diagonal gain matrix to amplify or reduce the commanded input (Landis and Crassidis, 2014). The components of the PWPF include a Schmidt trigger, a lag filter, and a feedback loop modulator (Sarma et al., 2010; Landis and Crassidis, 2014; Khosravi and Sarhadi, 2016). The filter contains the time constant gain $\boldsymbol{\tau}_m \in \mathbb{R}^{3\times3}$ and gain matrix $\boldsymbol{K}_m \in \mathbb{R}^{3\times3}$. The Schmidt trigger is an on/off relay with a dead band and hysteresis. V_{on} and V_{off} are the switching thresholds and V_m and $-V_m$are the output thrust levels for the Schmidt trigger. If the error is defined by $\boldsymbol{e}(t) = \boldsymbol{s}(t) - \boldsymbol{v}(t)$, the control law can be:

$$\boldsymbol{f}(t) = \boldsymbol{f}(0) + [\boldsymbol{K}_m\boldsymbol{e} - \boldsymbol{f}(0)]\left(1 - \boldsymbol{e}^{-t/\boldsymbol{\tau}_m}\right) \tag{37}$$

The parameters of the PWPF modulator are obtained in a similar way to (Landis and Crassidis, 2014) and are shown in Table 3.

5. Simulation study

For this analysis, the spacecraft parameters are selected from (Curti et al., 2010). To validate the proposed approach, we used MATLAB/Simulink to design and test the landing strategy shown in Fig. 7. Table 4 shows the initial state of the spacecraft in addition to the data necessary for the calculation of parameters of force and acceleration, including the feedback gains in the control PD and threshold of the PWPF.

Table 3
Recommended ranges for PWPF parameters.

Parameter	Static	Dynamic	Recommended
K_m	$2 < K_m < 7$	N/A	$2 < K_m < 7$
τ_m	$0.1 < \tau_m < 1$	$0.1 < \tau_m < 0.5$	$0.1 < \tau_m < 0.5$
V_{on}	$V_{on} > 0.3$	N/A	$V_{on} > 0.3$
V_{off}	$V_{off} < 0.8V_{on}$	N/A	$V_{off} < 0.8V_{on}$
K_{pm}	N/A	$K_{pm} \geq 20$	$K_{pm} \geq 20$

5.1. Case 1: Non-zero initial velocity

Tau-coupling landing strategy can be used when the spacecraft is to land after deorbiting and the initial velocity is not necessarily null. Fig. 8 show the landing-controlled position, velocity respectively, the motion of z-axis is coupled with the motion of x and y-axis to reach the target. The evolution of the trajectory is also properly tracked. The switching control signal required by the thrusters is calculated by the PWPF (Fig. 6) and depicted in Fig. 9.

The three-dimensional representation for optimal and non-optimal landing controlled-trajectory using Tau-coupling strategy is shown in Fig. 10.

5.2. Case 2: Zero initial velocity

A time-history position and velocity trajectory planned and controlled designed using intrinsic-tau strategy is shown in Fig. 11. The trajectory reaches the desired position, denoted with a green point and the velocity at the end of the maneuver is zero. The switching control signals for the thrusters are also determined and shown in Fig. 12.

In order to see more details of the on-off thruster profile, a closed look of Fig. 9 was generated (Fig. 13). The thrust profiles in Figs. 9 and 12 can be achieved by currently available thrusters, for example, the MR-L106 of Aerojet Rocketdyne.

Fig. 14 shows the Intrinsic-Tau trajectory planned and controlled landing in the three-dimensional space, the trajectory can be modified by adjusting the k values to reduce the gaps in the guided movements.

Table 4
Simulation parameters.

Spacecraft initial state		
$x_0\ y_0\ z_0$	622 850 1450	(m)
$x_n\ y_n\ z_n$	231.6 86.17 211.7	(m)
Case 1 : $\dot{x}_0\ \dot{y}_0\ \dot{z}_0$	0 0–3.3	(m/s)
Case 2 $\dot{x}_0\ \dot{y}_0\ \dot{z}_0$	0 0 0	(m/s)
$k_{xz}\ k_{yz}\ k_z$	1 1 0.3127	–
$k_{xg}\ k_{yg}\ k_{zg}$	0.2205 0.2205 0.2205	–
Spacecraft parameters		
m_{sc}	500	(kg)
Ixx Iyy Izz	427 354 260.4	(kg m^2)
T	20	N
Asteroid Parameters		
C_{20}	-4.9793×10^{-5}	–
C_{22}	2.0416×10^{-5}	–
μ	2.8694	m^3/s^2
PD-Control Gains		
$K_{px}\ k_{py}\ k_{pz}$	0.22 0.29 0.37	–
$K_{vx}\ k_{vy}\ k_{vz}$	4.3 3.3 2.3	–
PWPF Parameters		
$k_{mx}\ k_{my}\ k_{mz}$	4.5 4.5 4.5	–
$\tau_{mx}\ \tau_{my}\ \tau_{mz}$	0.15	–
$V_{onx}\ V_{ony}\ V_{onz}$	0.45	–
$V_{offx}\ V_{offy}\ V_{offz}$	0.35	–
$k_{pmx}\ k_{pmy}\ k_{pmz}$	350,000 350,000 350,000	–

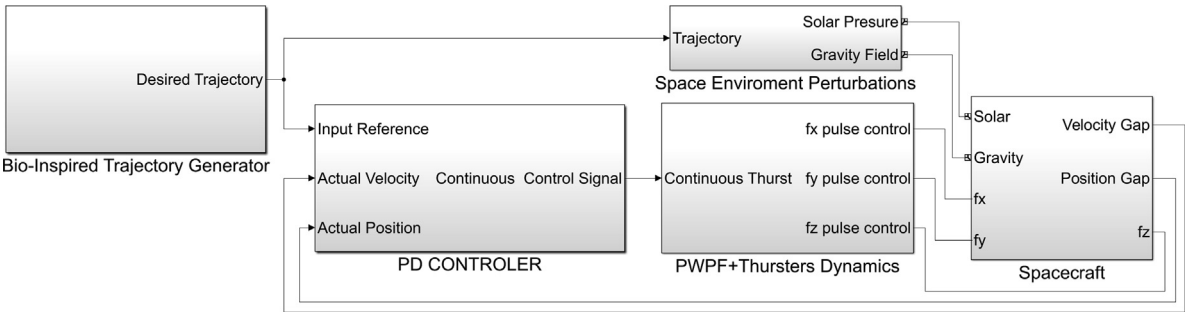

Fig. 7. Overall Bio-inspired guidance and control strategy in Simulink™ environment.

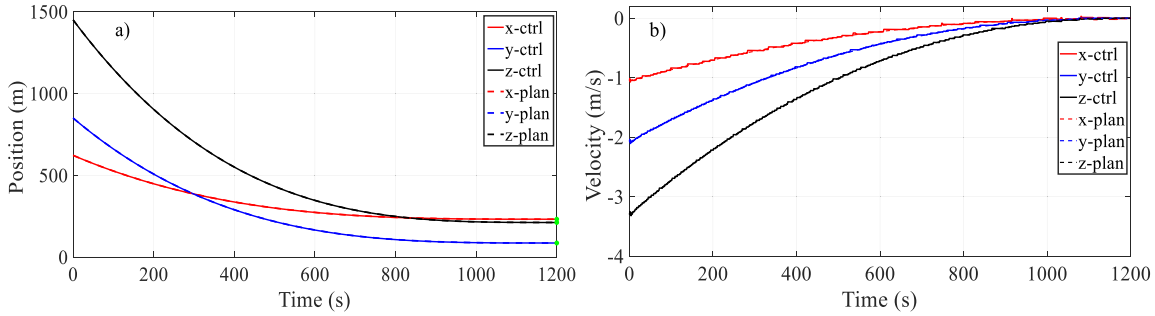

Fig. 8. Time-history: (a) position and (b) velocity trajectory, optimal Tau-coupling strategy.

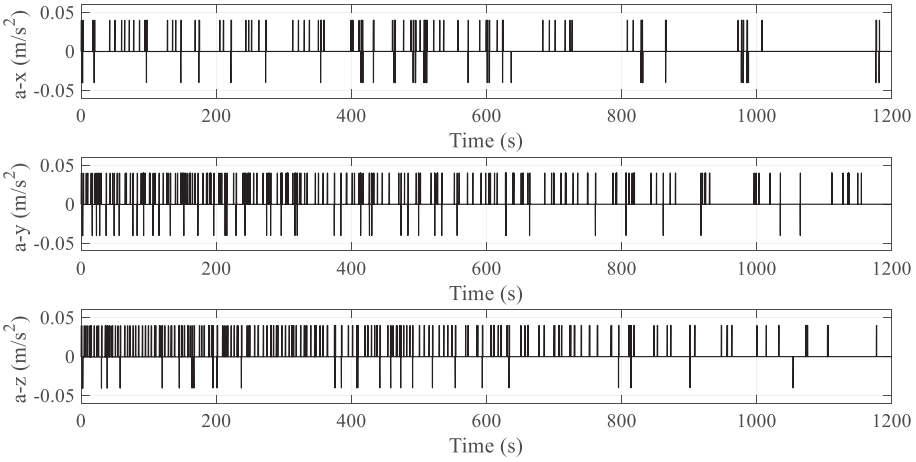

Fig. 9. Spacecraft acceleration, optimal Tau-coupling strategy.

In both cases, application of the Tau theory previously described for the design of the landing trajectory, a final velocity equal to zero is assumed. However, previous missions mentioned in Dunham et al. (2002) show the application of final velocity on the landing contact. If, for mission needs, a non-zero contact velocity is required, an improved version of the intrinsic-Tau strategy called "Tau-G improved" may be applied (Yang et al., 2016).

Additionally, research work carried out in Curti et al. (2010) shows an analysis and experimentation for the selection of thruster's for the control of a spacecraft in close proximity operations on a celestial body, the numerical and experimental results are similar to the switching control signals for the thrusters shown in this research paper. In Furfaro and Wibben (2013) a PWPF module is included in the Guidance Navigation Control (GNC) architecture for the implementation of Multiple Sliding Surfaces Guidance (MSSG) techniques, in the same way the acceleration plots about command histories generated by the MSSG algorithm show similar results to those shown in Figs. 9 and 12 in this work. Both, Curti et al. (2010) and Furfaro and Wibben (2013) navigation sensors such as LIDAR, Cameras, Inertial Measurement Unit (IMU) and Star Tracker are proposed, which are necessary elements

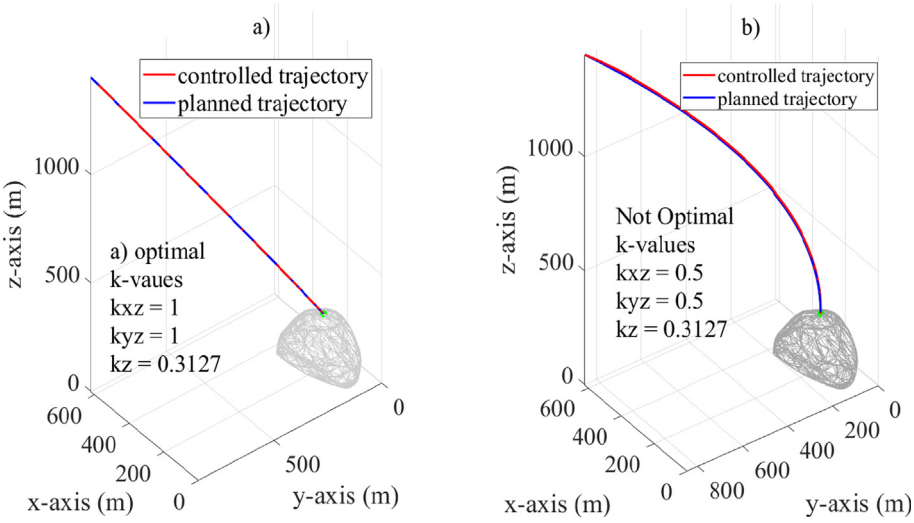

Fig. 10. Planned and controlled, (a) optimal and (b) non-optimal 3D trajectory Tau-coupling strategy.

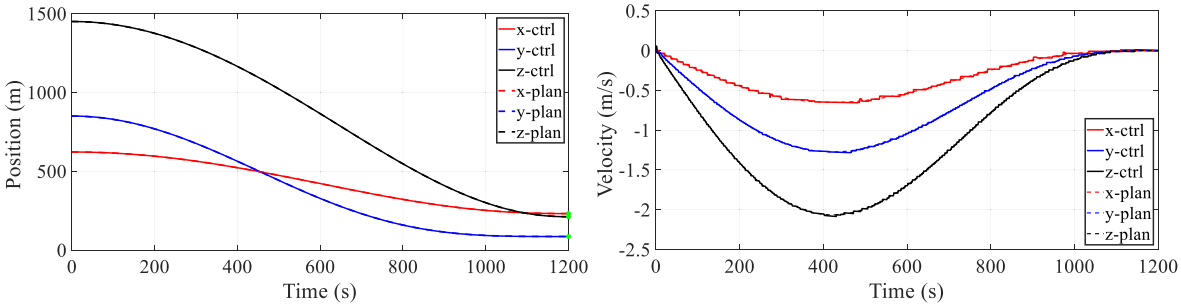

Fig. 11. Time-history: (a) position and (b) velocity trajectory, optimal intrinsic-Tau strategy.

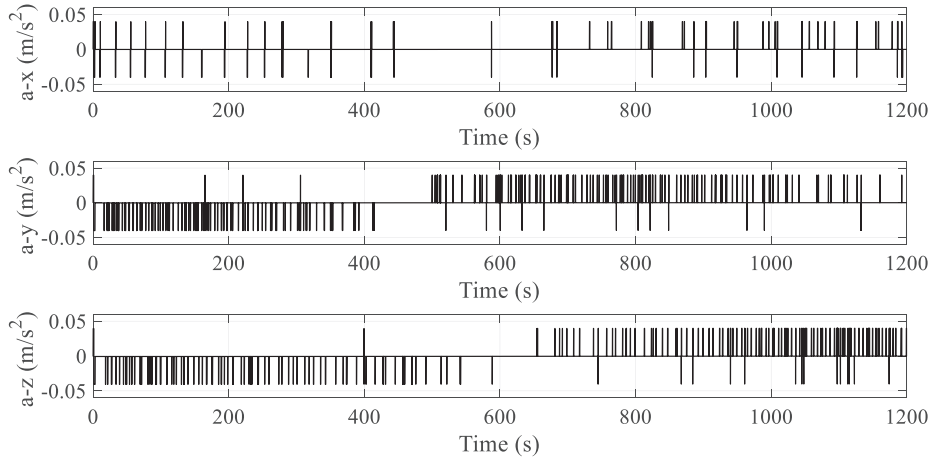

Fig. 12. Spacecraft Acceleration, optimal intrinsic-Tau Strategy.

for a GNC system to function properly. This research work focuses on showing an alternative method of planning for a soft and slow landing on an asteroid and space navigation for which based on the fundamental principles 1 and 2 of the Tau theory, the closing control of the action gaps suggests that the movement requires sensoring between the initial conditions and the end-effector (landing target).

6. Comparative analysis and discussion

In this section, the Tau coupling-guided trajectory is compared with a commonly used technique such as the cubic spline. For this purpose, the case where an initial residual velocity exists is studied. Different initial velocities will be assigned to the spacecraft to analyze the behavior of both methods. Changes in the planned velocities can hap-

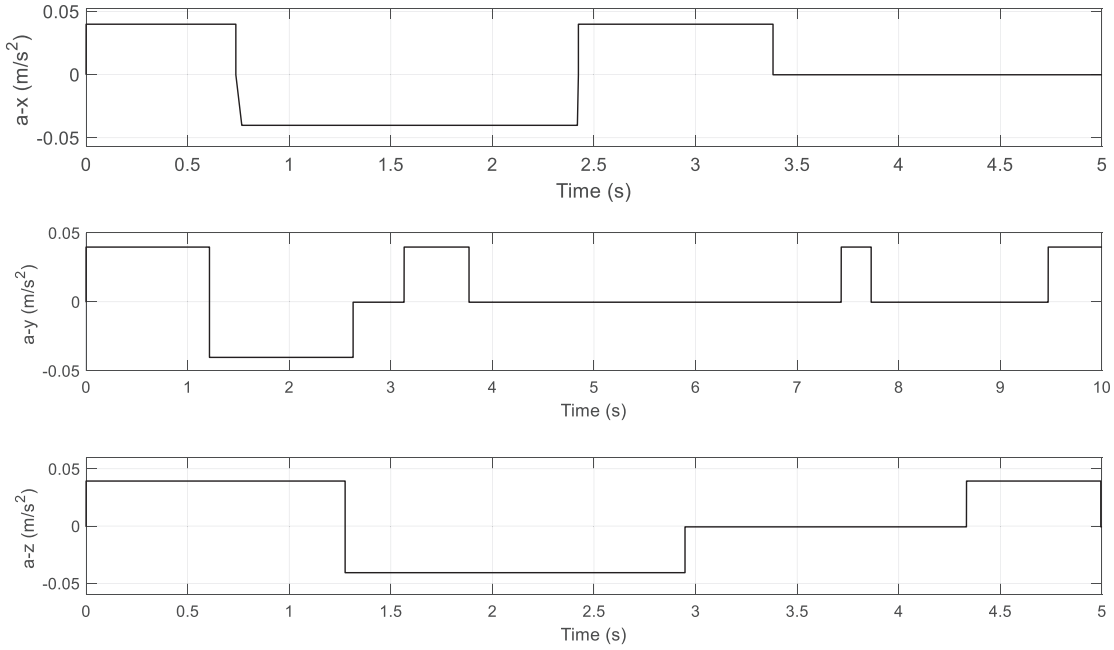

Fig. 13. Zoom-in into the acceleration profile of the Tau-coupling strategy to observe on-off details.

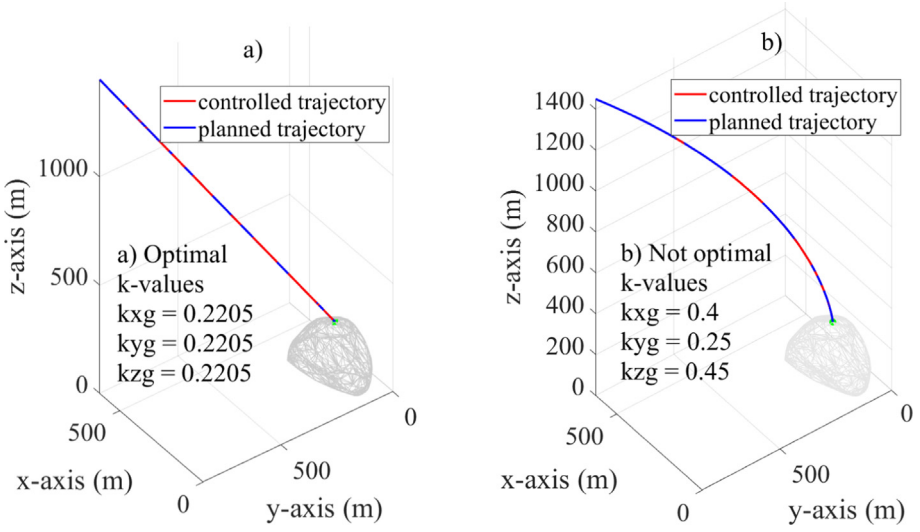

Fig. 14. Planned and controlled, (a) optimal and (b) non-optimal 3D trajectory intrinsic-Tau strategy.

pen due to small measurement errors, sensors' resolution and deviations from the planned initial state. Fig. 15 shows the trajectory described by the spacecraft under cubic polynomial path planning when the initial velocity in the vertical direction is modified.

Note that the position goes below zero at some point, which means the spacecraft would imminently collide with the asteroid and consequently the mission would fail. this can also be corroborated with the velocity graph, which indicates that the velocity crosses the zero much time before the end of the maneuver.

Now, recalling the case shown in Fig. 8a and b but suppose that the velocity is modified to be -5.3 m/s in z-direction. If no change is made to adjust the trajectory the spacecraft will collide with the asteroid as shown in Fig. 16a and b. However, in these case Tau theory is used to plan the landing trajectory and as shown in Fig. 16c and d, the final planned landing point is reached with zero velocity, demonstrating that it is possible to attain soft landing even when deviations from the intended initial state occurs. Additionally, a change in the parameters (position and velocity) of landing at time t during the descent can be easily modified if a serious deviation occurs.

The bio-inspired trajectory proposed here assumes that close-range rendezvous has been performed, the satellite is hovering near to the surface of the asteroid, and the control forces generated by the actuators are bigger in several orders than the space environment disturbances, to focus

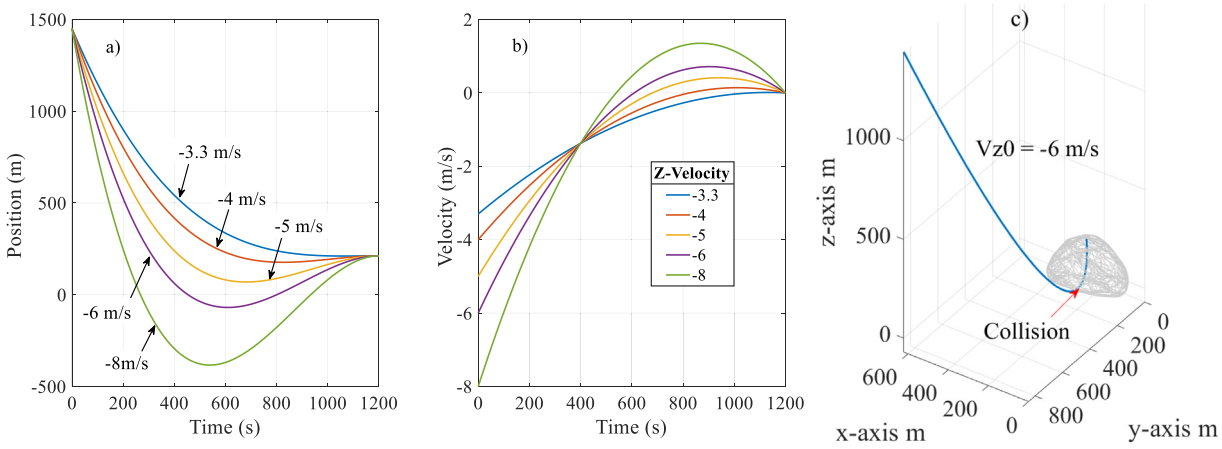

Fig. 15. Landing position and velocity on cubic polynomial strategy, z-change due to speed rate.

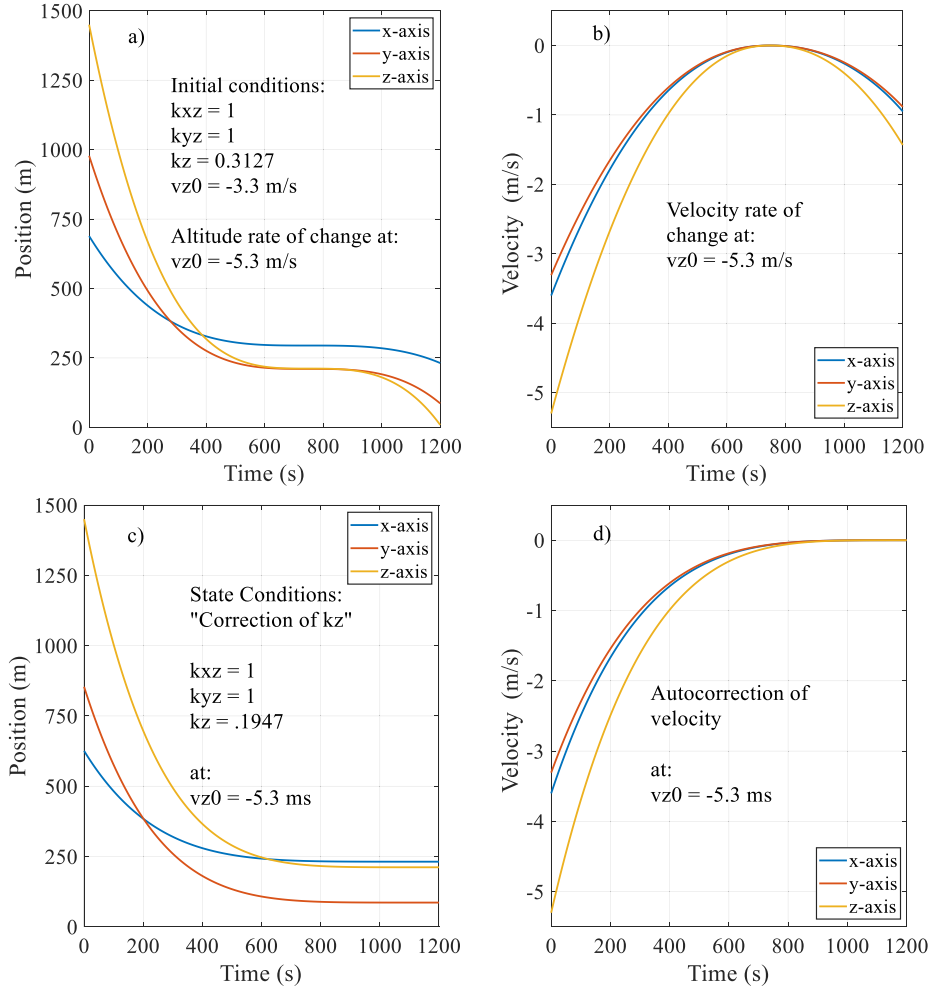

Fig. 16. Landing position and velocity (a-b) uncorrected, (c-d) corrected on Tau-coupling strategy.

our work in the guidance method. Because of such considerations, some effects of the orbital mechanics are not treated with detail and toughness in this work. However, when designing the trajectory, special attention should be paid to significant facts such as a proper selection of starting and landing spots as some orbits and regions may be more stables than others or require less energy to perform the maneuver; the complex dynamics and nonlinearities of the outer space environment, the influence of surrounding bodies; the irregular shape and unknown parameters of the celestial bodies; the noise and errors generated in the sensory system; and the performance limitations and power

requirements of the available technology. Lack of attention in those aspects may lead to a failed mission as small errors or deviations may cause an undesired collision, especially if the trajectory is planned off-line and there are not on-line feedback adjustment mechanisms.

Another aspect to consider is that the introduced method requires the use of an active propulsion system to enable tracking of the bio-inspired trajectory and correct for deviations, as well as a vision-based guiding sensory system to provide the spacecraft with information of its state, including position, velocity and acceleration, and the distance from the landing point. Adding sensors and actuators to the spacecraft should be always done cautiously and considering proper mass and volume budgeting allocation as any hardware addition will also increase the mass, volume and complexity of the satellite system.

7. Conclusions

This paper demonstrates the feasibility of using the Tau theory for trajectory generation to achieve a soft landing on the surface of asteroids. It was illustrated that Tau theory can be used to design a trajectory both from hovering and after deorbiting initial states. The introduced study, included the validation of the proposed approach in a 3D environment subject to external disturbances such as the solar pressure and gravity gradient influence, a continuous closed-loop controller and the corresponding switching control that will directly actuate the spacecraft thrusters by means of a PWPF modulators, which in the future would allow proper actuators selection. Some advantages of the method have been identified. The objective of the study that consisted of determining if bio-inspired approaches can be successfully applied in outer space tasks, given the fact the human beings and some other living agents are highly skilled and adaptable to different environments, was achieved. Because tau theory demonstrated to be capable of being used on closed-proximity operations, considering the particular case of asteroid landing. It was also shown that the method offers some advantages; for example, it is simple in complexity, as only one single constant, the tau constant k, can modify the kinematic behavior of the landing trajectory, this is important in close proximity operations, as sometimes it may be desired to reach the final destination with zero velocity or a small velocity, some others, landing with a predefined final velocity can be considered. Another advantage is that it can easily accommodate changes in the initial conditions, which may change due to several factors such as errors or deviations from sensors, the under performance of the controller and unplanned maneuver changes. Lastly, but not least, tau theory allows closing different gaps at the same time precisely and with the same simple formulation, just by correctly selecting the tau-coupling constant. Therefore, the method demonstrated to be applicable, simple, can cope with different mission scenarios, unexpected changes in the initial settings, and opens new opportunities to think about the use of bio-inspiration in outer space applications.

Declaration of Competing Interest

The authors declare that they have no known competing financial interests or personal relationships that could have appeared to influence the work reported in this paper.

References

Accomazzo, A., Derri, P., Lodiot, S., et al., 2017. The final year of the Rosetta mission. Acta Astronaut. 136, 354–359. https://doi.org/10.1016/j.actaastro.2017.03.027.

AlandiHallaj, M., Assadian, N., 2017. Soft landing on an irregular shape asteroid using multiple-horizon multiple-model predictive control. Acta Astronaut. 140, 225–234. https://doi.org/10.1016/j.actaastro.2017.08.019.

Balmino, G., 1994. Gravitational potential harmonics from the shape of a homogeneous body. Celest. Mech. Dyn. Astr. 60, 331–364. https://doi.org/10.1007/BF00691901.

Biele, J., Ulamec, S., Maibaum, M., et al., 2015. The landing(s) of Philae and inferences about comet surface mechanical properties, Science 349, 6247 aaa9816. http://science.sciencemag.org/content/349/6247/aaa9816/tab-pdf.

Curti, F., Romano, M., Bevilacqua, R., 2010. Lyapunov-based thrusters' selection for spacecraft control: analysis and experimentation. J. Guid. Control Dynam. 33 (4). https://doi.org/10.2514/1.47296.

Cheng, L., Wang, Z., Jiang, F., 2019. 2019, 'Real-time control for fuel-optimal Moon landing based on an interactive deep reinforcement learning algorithm'. Astrodynamics 3, 375–386. https://doi.org/10.1007/s42064-018-0052-2.

Dawkins P., 2003–2020. Calculus III/3-Dimensional Space/Arc Length with Vector Functions. http://tutorial.math.lamar.edu/Classes/CalcIII/VectorArcLength.aspx.

Dunham, D.W., Farquhar, R.W., McAdams, J.V., et al., 2002. Implementation of the first asteroid landing. Icarus 159, 433–438. https://doi.org/10.1006/icar.2002.6911.

Ferrari, F., Lavagna, M., Howell, K.C., 2016. Dynamical model of binary asteroid systems through patched three-body problems. Celest. Mech. Dyn. Astr. 125 (4), 413–433. https://doi.org/10.1007/s10569-016-9688-x.

Ferrari, F., Lavagna, M., 2018. Ballistic landing design on binary asteroids: the AIM case study. Adv. Space Res. 62 (8), 2245–2260. https://doi.org/10.1016/j.asr.2017.11.033.

Frieger, G., 2013–2020. 3D Asteroid Catalogue, Asteroid (99942). https://3d-asteroids.space/asteroids/99942-Apophis.

Furfaro, R., Wibben, D.R., 2013. Asteroid precision landing via multiple sliding surfaces guidance techniques. J. Guid. Control Dynam. 36 (4), 1075–1092. https://doi.org/10.2514/1.58246.

Huang, X., Cui, H., Cui, P., 2004. An autonomous optical navigation and guidance for soft landing on asteroids. Acta Astronaut. 54 (10), 763–771. https://doi.org/10.1016/j.actaastro.2003.09.001.

Ivashkin, V.V., Stikhno, C.A., 2009. On the use of the gravitational effect for orbit correction of the asteroid apophis. Doklady Phys. 54 (2), 101–105. https://doi.org/10.1134/S1028335809020141.

Ivashkin, V.V., Lang, A., 2017. Analysis of the orbital motion of the asteroid apophis' Satellite. Cosmic Res. 55 (4), 253–262. https://doi.org/10.1134/S0010952517030054.

Kelly, R., Santibañez, V., Loria, A., 2005. Control of Robots Manipulators on Joint Space. Springer, Germany.

Kendoul, F., Ahmed, B., 2010. Bio-inspired TauPilot for automated aerial 4D docking and landing of unmanned aircraft systems. In: Paper Published at 2012 IEEE/RSJ International Conference on Intelligent Robots and Systems, pp. 480–487. https://doi.org/10.1109/IROS.2012.6385586.

Kendoul, F., 2013. Four-dimensional guidance and control of movement using time-to-contact: application to automated docking and landing of unmanned rotorcraft system. Int. J. Robot. Res. 33 (2), 237–267. https://doi.org/10.1177/0278364913509496.

Khosravi, A., Sarhadi, P., 2016. Tuning of pulse-width pulse-frequency modulator using PSO: an engineering approach to spacecraft attitude controller design. Automatika 57 (1), 212–220. https://doi.org/10.7305/automatika.2016.07.618.

Lan, Q., Li, S., Yang, J., Guo, L., 2014. Finite-time soft landing on asteroids using nonsingular terminal sliding mode control. Trans. Inst. Meas. Control 36 (2), 216–223. https://doi.org/10.1177/0142331213495040.

Landis, Markley F., Crassidis, J.L., 2014. Fundamentals of Spacecraft Attitude Determination and Control. Springer, New York Heidelberg Dordrecht London, p. 2014.

Lantoine, G., Braun, R.D., 2006. 'Optimal Trajectories for Soft Landing on Asteroids, Space Systems', Design Lab., Georgia Inst. of Technology, AE8900 MS Special Problems Report, Atlanta, GA, https://pdfs.semanticscholar.org/8295/2b6cdeadab6fbd758073a8012e8f45dce248.pdf.

Lauretta, D.S., Bartels, A.E., Barucci, M.A., et al., 2015. The OSIRIS-REx target asteroid (101955) Bennu: constraints on its physical, geological, and dynamical nature from astronomical observations. Meteorit. Planet Sci. 50 (4), 834–849. https://doi.org/10.1111/maps.12353.

Lee, D.N., 2009. General tau theory: evolution to date. Perception 38, 837–858. https://doi.org/10.1068/pmklee.

Lee, D.N., 1976. A theory of visual control of braking based on information about time-to-collision. Perception 5, 437–459. https://doi.org/10.1068/p050437.

Lee, D.N., 1998. Guiding movement by coupling Taus. Ecol. Psychol. 10 (3–4), 221–250. https://doi.org/10.1207/s15326969eco103&4_4.

Lee, D.N., Davies, M., Green, P., et al., 1993. Visual control of velocity of approach by pigeons when landing. J. Exp. Biol. 180, 85–104 http://jeb.biologists.org/content/180/1/85.article-info.

Li, S., Cui, P., Cui, H., 2006. Autonomous navigation and guidance for landing on asteroids. Aerosp. Sci. Technol. 10 (3), 239–247. https://doi.org/10.1016/j.ast.2005.12.003.

Li, Y., Wang, H., Zhao, B., Liu, K., 2015. Adaptive Fuzzy sliding mode control for the probe soft landing on the asteroids with weak gravitational field. Math. Probl. Eng. 2015, ID 582948. http://dx.doi.org/10.1155/2015/582948.

Liu, K., Liu, F., Wang, S., Li, Y., 2014. Finite-time spacecraft's soft landing on asteroids using PD and nonsingular terminal sliding mode control. Math. Probl. Eng. 2105, ID 510618. https://doi.org/10.1155/2015/510618.

NASA Jet Propulsion Laboratory/Solar System Dynamics/JPL Small-Body Database Browser/99942 Apophis (2004 MN4), 2005. https://ssd.jpl.nasa.gov/sbdb.cgi?sstr=99942;orb=1.

Pinson, R., Lu, P., 2015. 'Rapid Generation of Optimal Asteroid Powered Descent Trajectories Via Convex Optimization, NASA Technical Report Server, AAS/AIAA Astrodynamics Specialist Conference, August 10, 2015 - August 13, 2015; Vail, CO; United States. SEE 20150019529.

Pinson, R., Lu, P., 2018. Trajectory design employing convex optimization for landing on irregular shaped asteroid. J. Guid. Control Dynam. 41 (6), 1243–1256. https://doi.org/10.2514/1.G003045.

Pravec, P., Scheirich, P., Durech, J., et al., 2014. The tumbling spin state of (99942) Apophis. Icarus 233, 48–60. https://doi.org/10.1016/j.icarus.2014.01.026.

Santos, W.G., Prado, A., Oliveira, G., Santos, L., 2018. Analysis of impulsive maneuvers to keep around the asteroid $2001SN_{263}$. Astrophys. Space Sci. 63 (1), 11. https://doi.org/10.1007/s10509-017-3234-5, ID. 14.

Sarma, S., Kulkarni, A.K., Venkateswaralu, A., et al., 2010. Spacecraft dynamics modeling and simulation using matlab-simulink. In: Paper Presented at 3rd MATEIT Conference New Delhi, India, https://www.researchgate.net/publication/266139189.

Scheeres D.J., 2012. Orbital Motion in Strongly Perturbed Environments: Applications to Asteroid, Comet and Planetary Satellite Orbiters. Springer-Praxis, German, 2012.

Tardivel, S., Scheeres, D.J., 2013. Ballistic deployment of science packages on binary asteroids. J. Guid. Control Dynam. 36 (3), 700–709. https://doi.org/10.2514/1.59106.

Tardivel, S., Michel, P., Scheeres, D.J., 2013. Deployment of a lander on the binary asteroid (175706) 1996 FG3, potential target of the european MarcoPolo-R sample return mission. Acta Astronaut. 89, 60–70. https://doi.org/10.1016/j.actaastro.2013.03.007.

TheSkyLive, 2020. Asteroid 99942 Apophis/Orbital Elements. https://theskylive.com/apophis-info#skychart.

Tsuda, Y., Yoshikawa, M., Saiki, T., Nakazawa, S., Watanabe, Si, 2019. Hayabusa2–Sample return and kinetic impact mission to near-earth asteroid Ryugu. Acta Astronaut. 156, 387–393. https://doi.org/10.1016/j.actaastro.2018.01.030.

Veverka, J., Farquhar, B., Robinson, M., et al., 2001. The landing of the NEAR-Shoemaker spacecraft on asteroid 433 Eros. Nature 413, 390–393. https://doi.org/10.1038/35096507.

Wang, Y., Xu, S., 2015. 'Body-fixed orbit-attitude hovering control over an asteroid using non-canonical Hamiltonian structure. Acta Astronaut. 117, 450–468. https://doi.org/10.1016/j.actaastro.2015.09.006.

Yang, H., Baoyin, H., 2015. Fuel-optimal control for soft landing on an irregular asteroid. IEEE Trans. Aero. Elec. Syst. 51 (3), 1688–1697. https://doi.org/10.1109/TAES.2015.140295.

Yang, H., Bai, X., Baoyin, H., 2017. Rapid generation of time-optimal trajectories for asteroid landing via convex optimization. J. Guid. Control Dynam. https://doi.org/10.2514/1.G002170.

Yang, H., Li, S., 2020. Fuel-optimal asteroid descent trajectory planning using a lambert solution-based costate initialization. IEEE Trnas. Aero. Elec. Syst., doi: 10.1109/TAES.2020.2988625.

Yang, H., Li, S., Bai, X., 2019. Fast homotopy method for asteroid landing trajectory optimization using approximate initial costates. J. Guid. Control Dynam. 42 (3), 585–597. https://doi.org/10.2514/1.G003414.

Yang, H., Bai, X., Baoyin, H., 2017b. Finite-time control for asteroid hovering and landing via terminal sliding-mode guidance. Acta Astronaut. 132, 78–89. https://doi.org/10.1016/j.actaastro.2016.12.012.

Yang, Z., Fang, Z., Li, P., 2016. Descentralized 4D trajectory generation for UAVs based on improved intrinsic Tau guidance strategy. Int. J. Adv. Robot. Syst. 1, 1–13. https://doi.org/10.5772/63431.

Yano, H., Kubota, T., Miyamoto, H., 2006. Touchdown of the Hayabusa spacecraft at the Muses Sea on Itokawa. Science 312 (5778), 1350–1353. https://doi.org/10.1126/science.1126164.

Yoshimitsu, T., Kubota, T., Nakatani, I., 2006. MINERVA rover which become a small artificial solar satellite. In: Paper Presented at P20th Annual AIAA/USU Conference on Small Satellites, Utah State University. https://digitalcommons.usu.edu/smallsat/2006/All2006/27/.

Zezu, Z., Weidong, W., Litao, L., et al., 2012. Robust Sliding mode guidance and control for soft landing on small bodies. J. Franklin Inst. 349 (2), 493–509. https://doi.org/10.1016/j.jfranklin.2011.07.007.

Zhang, H., Cheng, B., Zhao, J., 2017. Extended Tau theory for robot motion control. In: Paper Published at CRA 2017 – IEEE International Conference on Robotics and Automation, pp. 5321–5326. https://doi.org/10.1109/ICRA.2017.7989626.

Zhang, Z., Xie, P., Ma, O., 2014. Bio-inspired trajectory generation for UAV perching movement based on Tau theory. Int. J. Adv. Robot. Syst. 11 (141). https://doi.org/10.5772/58898.

Zhenjiang, Z., Meng, Y., Hutao, C., Pingyuan, C., 2012. The method to determine spherical harmonic model of asteroid based on polyhedron. IPCSIT 53. https://doi.org/10.7763/IPCSIT.2012.V53.No.2.21.